ISSN 2176-5480

22nd International Congress of Mechanical Engineering (COBEM 2013)
November 3-7, 2013, Ribeirão Preto, SP, Brazil


# EXPERIMENTAL AND NUMERICAL STUDIES OF THE FLOW FIELD IN AN URBAN STREET CANYON

**Artur Burgo**
**Lizandra Broseghim Foeger**
**Reginaldo Rosa Cotto de Paula**
Sanitary and Environmental Engineering Department, IFES, Vitoria, E.S., Brazil
arturburgo@gmail.com
lizandra.bf@gmail.com
cottoreginaldo@gmail.com

**Fernanda Capucho Cezana**
Mathematical Department, IFES, Vitoria, E.S., Brazil
fecezana@ifes.edu.br

**Marcos Sebastião de Paula Gomes**
mspgomes@mec.puc-rio.br
Mechanical Engineering Department, PUC-Rio, Rio de Janeiro, R.J.

**Abstract**. *Experimental and numerical studies were used to investigate the effects of ambient wind on flow around a group of buildings. The idealized urban street canyon was formed with six cubical building models of the same size which were arranged in a symmetric configuration with two aspect ratios. A series of experimental measurements of wind velocity were made over an urban street canyon arrangement using a Pitot probe. Fluid modeling was done in an atmospheric boundary layer wind tunnel. The approach flow was directed perpendicular to the street axis. Results were compared to numerical simulations of the same configurations using the commercial code CFX 13.0. The effects of building spacing on wind flow were examined numerically by using standard κ-ε turbulence model. The numerical results using standard κ-ε turbulence model presented good predictive performance of the flow field in an urban street canyon.*

***Keywords:*** *Turbulence models, atmospheric boundary layer, urban region*

## 1. INTRODUCTION

The predictions of flow patterns caused by superposition and interaction of flow associated with buildings adjacent to another are of particular relevance for engineers, meteorologists and planners. Such interactions between flow and obstacles can provide information to be used in guidelines for optimizing of ventilation systems, ensuring sunlight, reducing heat island effects and for risk assessments of hazardous materials emitted to the atmosphere in urban regions (Kim and Baik, 2004). The aerodynamics and environmental characteristics of the flow within and above the urban region is classified in three regimes: isolated roughness flow; wake interference flow and skimming flow (Oke, 1988). These flow patterns are dependent on area density, arrangement of buildings; roughness geometry; distance between buildings and meteorological conditions, such as incident wind (Kim *et al*., 2012).

Flow patterns which develop in urban street canyons around groups of buildings govern the dispersion of pollutants, heat transfer, wind-loads and other scalars. The wind direction and the street geometry determine broad characteristics of the flow within and over the buildings. The three regimes between two rows of similar height buildings are characterized by: (1) Isolated roughness flow: when the building height to street width ratio, $H/W$ is less than 0.03 a flow similar to the flow around an isolated building develops; (2) Wake interference flow: this flow regime develops when $0.30 < H/W < 0.65$ and is prevalent in urban and suburban areas. It involves interaction of the building's wakes and their impingement on downwind buildings thusly resulting in a complicated flow and (3) Skimming flow: this flow regime develops when $H/W > 0.65$. This is a usual regime encountered in a city centre. Skimming flow is characterized by a re-circulation, which has been found not to exceed the building height (Oke, 1988).

Experimental and computational research of three-dimension flows has been applied to simulated urban flow (Gayev and Savory, 1999; Gromke and Ruck, 2007). These studies have contributed to our understanding of the complex structure of flow patterns, the effects of meteorological parameters and building arrangements on flow in urban street canyons (Vardoulakis *et al*., 2003). Meroney *et al*. (1996) reported a short review of the field and experimental studies of the flow and dispersion in urban regions. The authors identified many of the characteristics of street canyon circulation, roof top separation regions and elevated boundary layers.

Louka *et al*. (1998) carried out field experiments to investigate the turbulent flow in street canyons and its coupling to the turbulent flow above roofs. The results showed that the profile of the roofs significantly affects the re-circulation within the street. For wind parallel to the street the channeling regime was observed. Chang and Meroney (2003)

ISSN 2176-5480



investigated the influence of bluff body flow and transport from stationary point sources of pollutants in an idealized urban region. The flow and dispersion of gases were determined by FLUENT using four different RANS turbulence closure approximations and a model fire dynamics simulator using a large eddy simulation. Calculations were compared against wind tunnel experiments. Results of measurements and calculations showed that the dispersion of gases within urban street-canyon were essentially unsteady.

In the present study, a commercial code obtained from the Computational Fluid Dynamic (CFD) ANSYS CFX was used. The incompressible and viscous and stationary Navier-Stokes equations were solved using κ–ε turbulence model. The results of numerical wind vertical profile within and over the urban street canyon of the same configuration were compared using wind tunnel experiments. The present numerical investigation is aimed at analyzing the effect of obstacles on flow structures.

## 2. MATERIAL AND METHODS

### 2.1 Governing equations

For a steady-state, neutral flow the governing equations of an incompressible fluid with constant viscosity, based on the Reynolds-averaged Navier-Stokes approach are the continuity equation and the momentum equation:

$$\frac{\partial \overline{u}_i}{\partial x_i} = 0 \tag{1}$$

$$\frac{\partial\left(\overline{u}_i \overline{u}_j\right)}{\partial x_i} + \frac{\partial\left(\rho \overline{u_i' u_j'}\right)}{\partial x_i} = -\frac{\partial p'}{\partial x_i} + \frac{\partial}{\partial x_j}\left[\frac{\mu_{eff}}{\rho}\left(\frac{\partial \overline{u}_i}{\partial x_j} + \frac{\partial \overline{u}_j}{\partial x_i}\right)\right] \tag{2}$$

where $u_i'$ and $\overline{u}_i$ are the fluctuating and mean velocities in the $x_i$-direction ($i$ =1, 2, 3); $\mu_{eff}$ is the effective viscosity accounting for turbulence, $p$' is the modified pressure and ρ is the density of the fluid. The kinematic Reynods stress $\overline{u_i' u_j'}$ represents the turbulent fluxes of momentum. In the κ–ε model the eddy viscosity is given by:

$$\mu_{eff} = \mu + \mu_t \tag{3}$$

where $\mu_t$ is the turbulence viscosity. This turbulence model assumes that $\mu_t$ is the correlated to the turbulence kinetic energy, κ, and turbulence dissipation ratio, ε, by:

$$\mu_t = C_\mu \rho \frac{\kappa^2}{\varepsilon} \tag{4}$$

where $C_\mu$ = 0.09 is a constant. The turbulent kinetic energy and its turbulence dissipation rate are modeled from the differential transport equations, respectively

$$\frac{\partial\left(\rho u_j \kappa\right)}{\partial x_j} = \frac{\partial}{\partial x_j}\left[\left(\mu + \frac{\mu_t}{\sigma_\kappa}\right)\frac{\partial \kappa}{\partial x_j}\right] + P_\kappa - \rho\varepsilon + P_{\kappa b} \tag{5}$$

$$\frac{\partial\left(\rho u_j \varepsilon\right)}{\partial x_j} = \frac{\partial}{\partial x_j}\left[\left(\mu + \frac{\mu_t}{\sigma_\varepsilon}\right)\frac{\partial \varepsilon}{\partial x_j}\right] + \frac{\varepsilon}{\kappa}\left(C_{\varepsilon 1} P_\kappa - C_{\varepsilon 2}\rho\varepsilon + C_{\varepsilon 1} P_{\varepsilon b}\right) \tag{6}$$

where $C_{\varepsilon 1}$ = 1.44, $C_{\varepsilon 2}$ =1.92, $\sigma_\kappa$ =1.0 and $\sigma_\varepsilon$ =1.3 are constants. $P_{\kappa b}$ and $P_{\varepsilon b}$ are the influence of the buoyancy forces and $P_\kappa$ is the turbulence production due to viscous forces.

ISSN 2176-5480



### 2.2 – Numerical methods

A commercial CFD code (ANSYS CFX 13.0) was used to calculate the flow field around a group of buildings. The code solves three-dimensional Reynolds-average Navier-Stokes (RANS) equation using a second order scheme. The fluid was considered to be incompressible and Newtonian under steady-state flow.

Equations 1 and 2 were discretized and solved by a finite volume method based numerical solver for unstructured numerical grids. The computational domain was extended 12*H* (streamwise) × 9*H* (spanwise) 6*H* × (height), where *H* is building height. The computational domain is reported in Fig. 1.

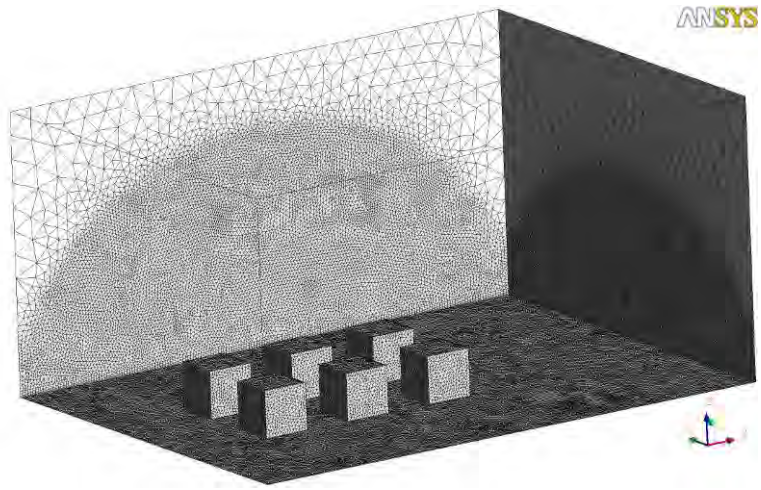


Figure 1. Computational domain and grid system.

### 2.3 – Boundary conditions

Inlet boundary conditions are presented in Tab. 1. The superior and lateral sides were designated to have free-slip boundary conditions, and the outflow side was designated as a pressure boundary. No-slip conditions were imposed on building surfaces and the ground.

Table 1. Inlet boundary conditions.

| |
|---|
| $\kappa$-$\varepsilon$ turbulence model |
| $\overline{u} \propto z^{0,45}$, $\overline{v} = \overline{w} = 0$ |
| $\kappa = 0,03u_{Hb}^2$, $\varepsilon = C_\mu^{3/4}\kappa^{3/2} \big/ kz$, $k$ = 0,41 and $C_\mu = 0,09$ |

### 2.4 The wind tunnel experiments

The flow considered in this work was investigated in open return wind tunnel with test section of 2.0 m × 0.5 m × 0.5 m, located at Energy Laboratory of IFES a Federal Institute of Technology of Espirito Santo, Vitoria, Brazil. Wood spires and roughness elements (cubical wooden blocks) were installed upwind of test area of the wind tunnel to generate a neutral atmospheric boundary layer (Irwin, 1981). The mean streamwise velocity has the following power law profile:

$$\frac{U(z)}{U_\delta} = \left(\frac{z}{\delta}\right)^p \tag{7}$$

where δ = 0.30 m is the atmospheric boundary layer thickness. In this work the velocity profile was fitted with $p$ = 0.30, which corresponds to the velocity profile over urban regions (Blessman, 1988). To study the effects of ambient wind on flow in an idealized urban area in the wind tunnel experiments there were used two columns with six cubical buildings of $H$ = 0.08 m, Fig. 2. These scale model buildings were arranged in a symmetric configuration with separation distances between buildings $W_2 = H$ and aspect ratio $H/W_2$ = 1.0. During the experiments the street width, $W_1$, was of the same value as the cube height. The main street was parallel to the oncoming wind flow with spacing between buildings perpendicular to it and the frontal area densities, $\lambda_f = [H \times B/(B + W_1)(B + W_2)$ = 0.5 and 0.11; were simulated. Measurements of the velocity vertical profile of wind were obtained with a Pitot-static tube with probe of 3 mm

ISSN 2176-5480



diameter (TSI EBT720). Figure 2 shows the localization of measured wind velocities at the top of buildings and center line of wind tunnel, these points were represented by $X_1$, $X_2$, $X_3$, $X_4$ and $X_5$.

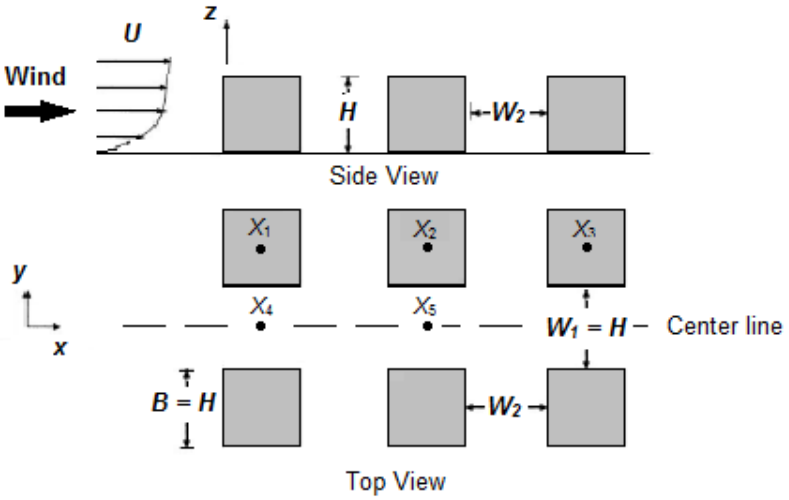


Figure 2. Schematic representation of urban street-canyon at $H/W_2$ = 1.0: model arrangement with cubical buildings.

## 3. RESULTS

In this work was initially performed a grid dependence study for six cubical buildings at $H/W_2$ = 1.0, using the standard κ-ε turbulence model and also evaluated were the numerical results of the wind vertical profile obtained from wind tunnel data. Figure 3 shows the comparison of the mean velocity vertical profiles obtained by numerical simulation and wind tunnel measurements at the top of buildings. For wind vertical profiles, at points $X_1$, $X_2$ and $X_3$, the numerical prediction using the κ -ε turbulence model presented good agreement with the measured values. However, near the top of the computational domain data the wind velocities were over-predicted in comparison with measured data. These results suggested that the flow was faster than it should be.

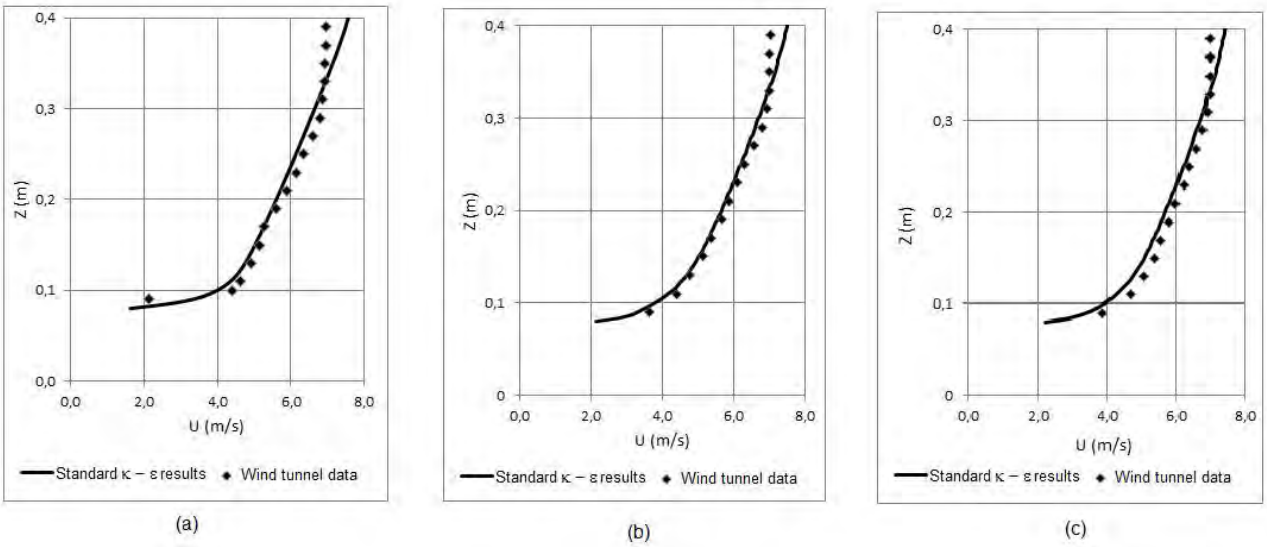


Figure 3. Street canyon at $H/W_2$ = 1.0: Validation of wind velocity vertical profiles numerical results against experimental data at the top of buildings for different points: (a) $X_1$ = 2.5 $H$ (first building); (b) $X_2$ = 4.5 $H$ (second building) and (c) $X_3$ = 6.5 $H$ (third building).

Figure 4 presents the comparison of wind velocity vertical profiles of experimental data and numerical results in the center line of the urban street canyon, $H/W_2$ = 1.0, for two different points, $X_4$ = 2.5 $H$ and $X_5$ = 4.5 $H$. According to Fig. 4a, the numerical vertical profile of velocity along the street centerline at $X_4$ = 2.5 $H$ at $z$ < 0.08 m was over-predicted by the standard κ-ε turbulence model and at $z$ > 0.10 m, the mean wind velocities were under-predicted. Figure 4.b shows that the numerical data of wind velocities along the street centerline at $X_5$ = 4.5 $H$ were under-predicted along the z axis. These results suggest that near the ground mean velocities computed were more liable to vary than the velocities measured.

ISSN 2176-5480



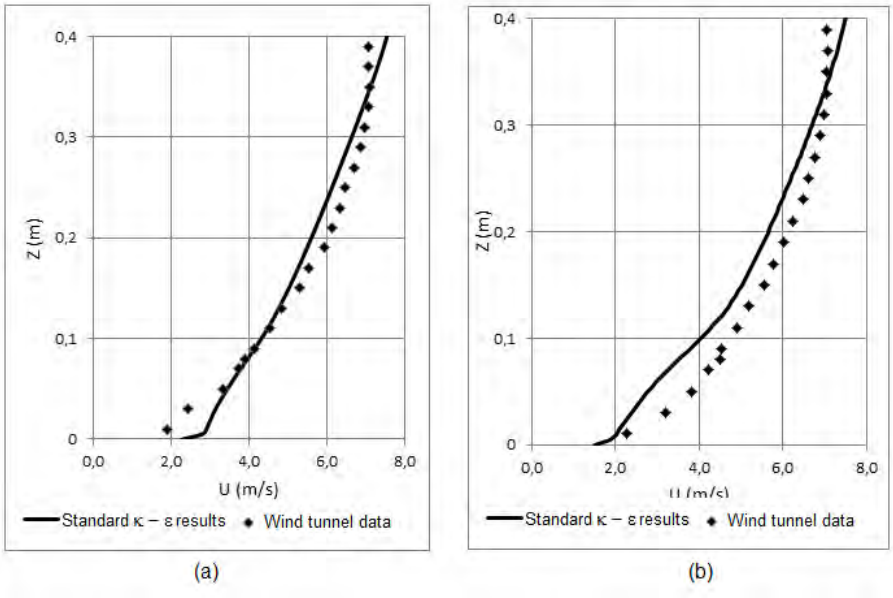


Figure 4. Street canyon at $H/W_2$ =1.0: Validation of wind velocity vertical profiles numerical results against experimental data at the centerline of urban street canyon for different points: (a) $X_4$ = 2.5 $H$ and (b) $X_5$ = 4.5 $H$.

Figures 5 and 6 show the velocity field obtained by the numerical simulation on the $x$-$z$ plane for the street canyon at $H/W_2$ = 1.0 and 0.5, respectively. The vertical recirculation behind the buildings can be seen in Fig. 5. Comparing the velocity field for different canyon spacing at $H/W_2$ = 1.0 and 0.5, it turned out that there was no fundamental change in the wind field, both numerical results exhibit the vertical recirculation behind buildings. But the dimensions of the same flow region changed. The results showed that flow within canyon space was decoupled from flow above top of building, which is characterized as skimming flow. However, the standard κ-ε turbulence model was not able to capture the reattachment point on the roof of first building in both urban canyon arrangements.

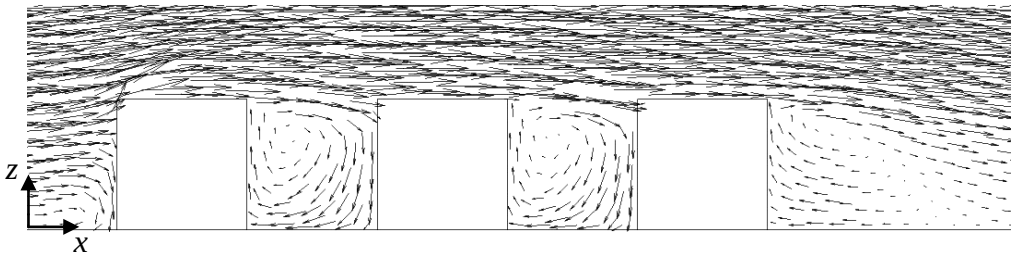


Figure 5. Side view of the street canyon at $H/W_2$ =1.0: Mean velocity vectors on the $x$-$z$ plane at $y$ = 5.5 $H$ .

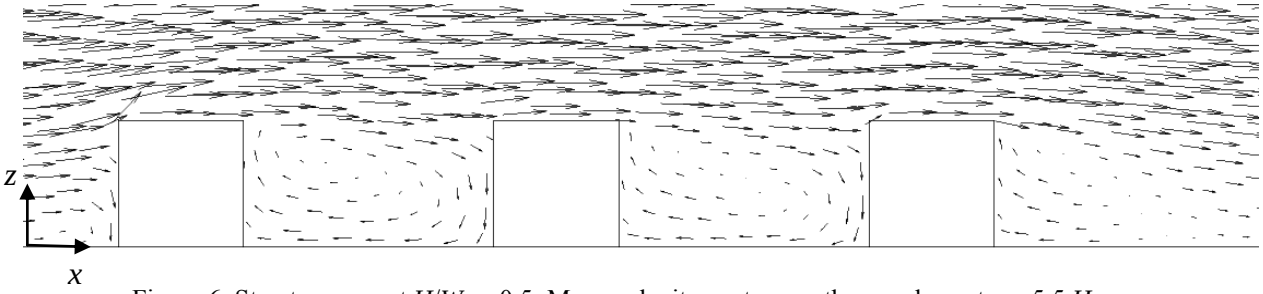


Figure 6. Street canyon at $H/W_2$ = 0.5: Mean velocity vectors on the $x$-$z$ plane at $y$ = 5.5 $H$ .

Figure 7 and 8 show the velocity field obtained by numerical simulation on the $x$-$y$ plane. The main street acts as a channel for the approaching wind when the stream-wise velocity is large in comparison with that of the secondary streets (canyons).The formation of a channeling effect due to the increase of the flow field in the first passage between the obstacles are clearly shown in the Figs. 7 and 8. The simulated boundary layer display near wake region behind the last building, see Figs. 7 and 8.

ISSN 2176-5480



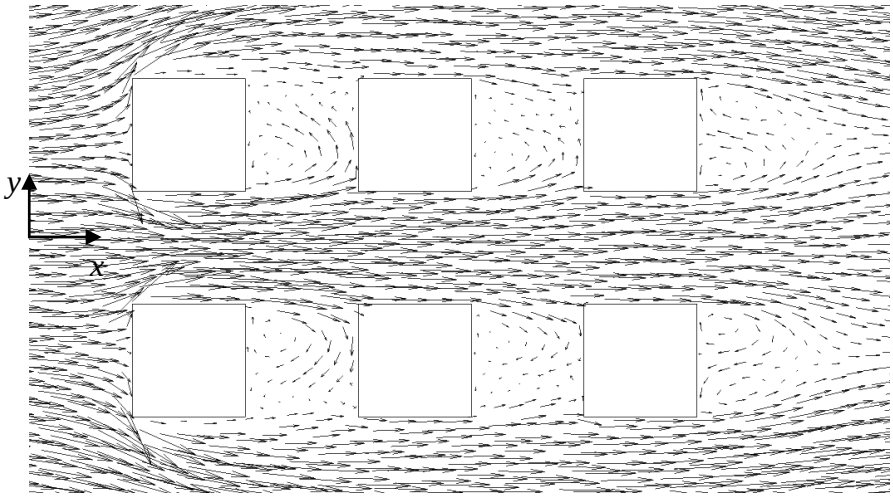


Figure 7. Street canyon at $H/W_2$ : Mean velocity vectors in $x$-$y$ plane at $z = 0.5H$.

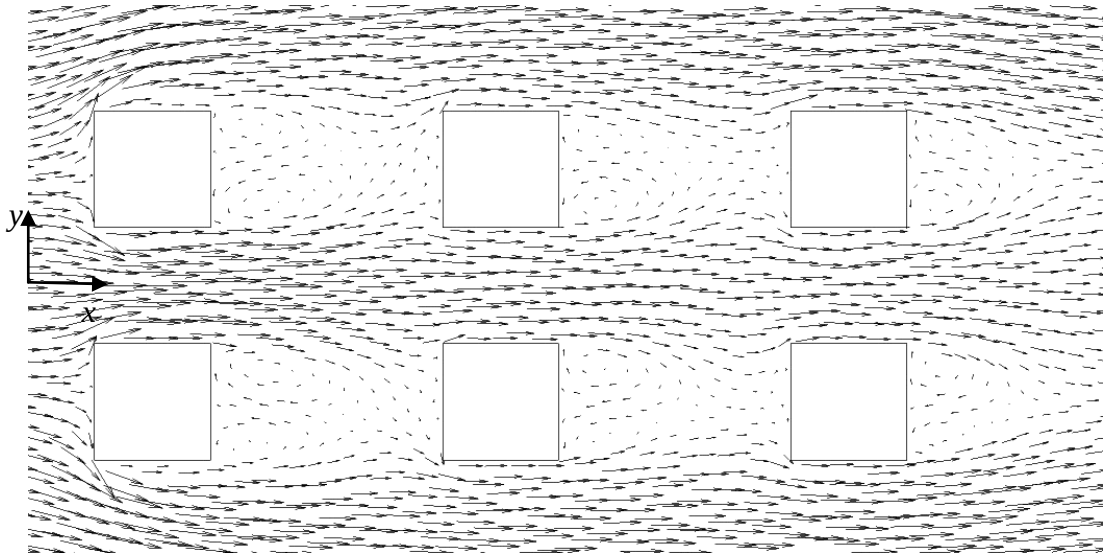


Figure 8. Street canyon at $H/W_2$ =0.5: Mean velocity vectors on the $x$-$y$ plane at $z = 0.5H$.

Figures 9 and 10 show the mean velocity streamlines on the $x$ -$z$ plane for the street canyons at $H/W_2$ = 1.0 and 0.5, respectively. The numerical results simulate well the standing vortex in front of the first building. In the numerical data this important characteristic of the incident flow in the urban region was captured. However the κ-ε failed to predicted the reattachment point and recirculation on the roof of the first building. In both canyon space was observed the formation of a unique counterclockwise rotating vortex, see Figs 9 and 10. The core vortex was located above and upstream of the canyon center. This formation of a large unique vortex behind the obstacles is characterized as skimming flow, as reported by Oke (1988).

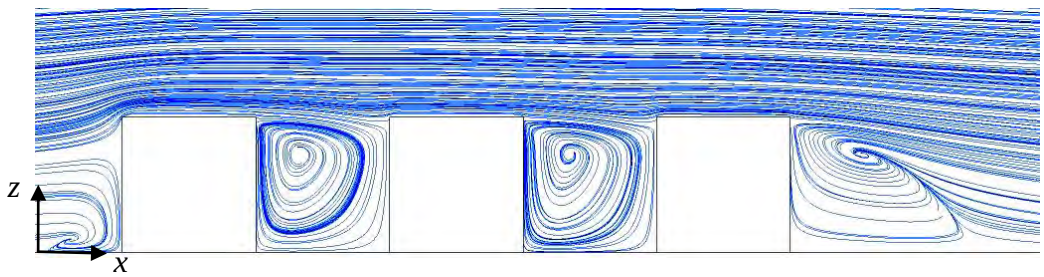


Figure 9. Street canyon at $H/W_2$ = 1.0: Mean velocity streamlines on the $x$-$z$ plane at $y$ = 5.5 $H$.

ISSN 2176-5480



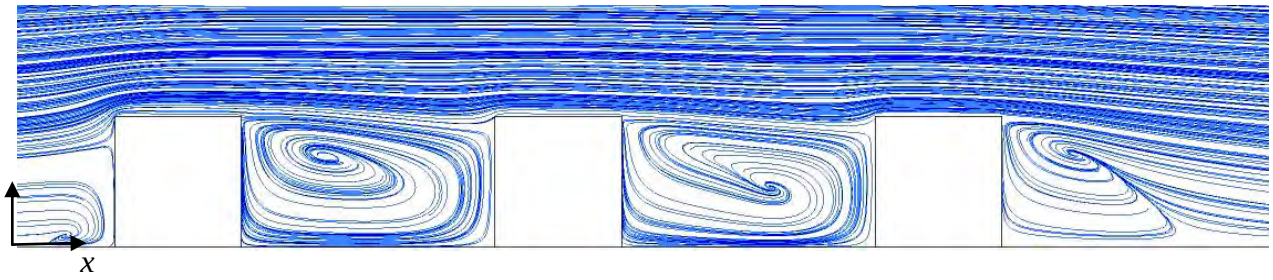


Figure 10. Street canyon at $H/W_2$: Mean velocity streamlines on the $x$-$z$ plane at $y$ = 5.5 $H$.

Figures 11 and 12 show the mean velocity streamline for street canyons on the $x$-$y$ plane at $H/W_2$ = 1.0 and 0.5, respectively. The numerical results showed the influence of building intersection on the flow field. The flow separates at the upstream corner of the obstacle leading to the formation of a recirculation zone in the side streets. Behind the first row of buildings was formed one recirculation zone and then, behind the second row of buildings were formed two recirculation zones. The recirculation zone formed behind the leeward wall of the last building has been predicted, as shown in Figs. 11 and 12.

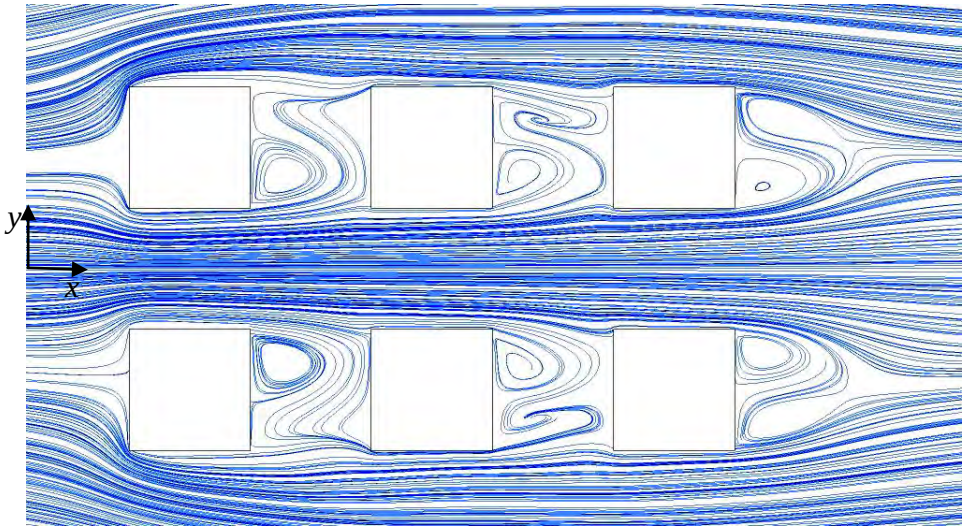


Figure 11. Street canyon at $H/W_2$ : Mean velocity streamlines on the $x$-$y$ plane at $z$ = 0.5 $H$.

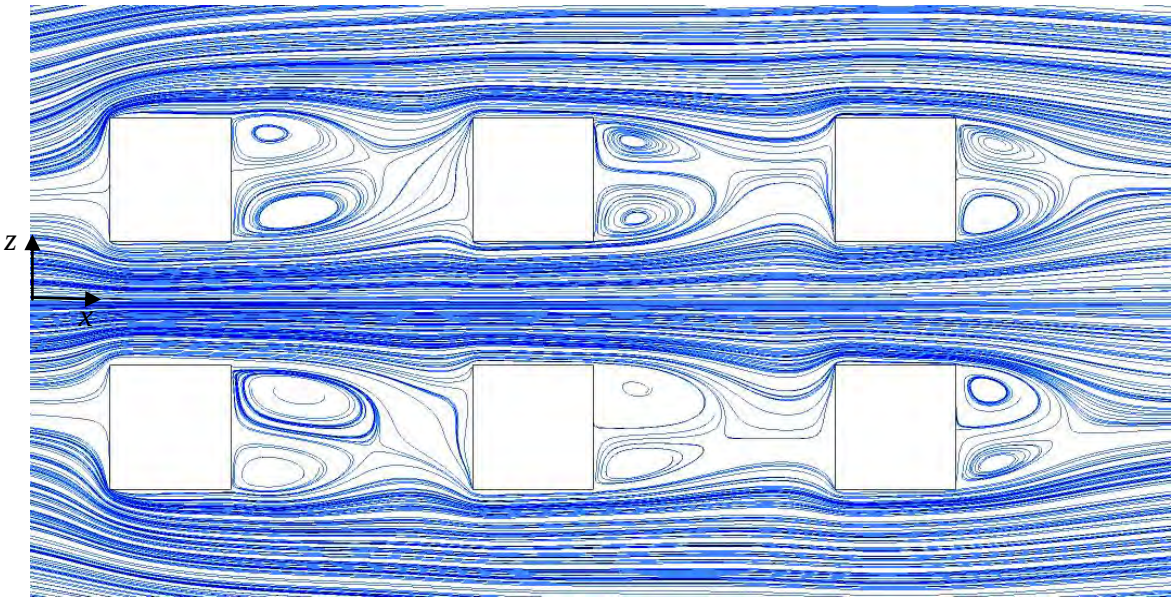


Figure 12. Street canyon at $H/W_2$ : Mean velocity streamlines on the $x$-$y$ plane at $z$ = 0.5 $H$.

ISSN 2176-5480



## 4. CONCLUSIONS

In this work the κ-ε turbulence model has been used to investigate the wind turbulence flow within an idealized urban street canyon. It is found that the performance of this turbulence model was generally good, in that most of the qualitative features of a skimming turbulent flow field within street canyon space were correctly reproduced. The comparison of predicted numerical results and measured mean velocity vertical profiles was also fairly good. The standard κ-ε turbulence model with an isotropic and linear viscosity, despite its simplicity, presented a good predictive performance on flow simulation of wind field in an urban street canyon. Thus, this model may be useful as a tool to evaluate the urban flow since it is simple to execute numerically without the need for excessive computation time.

## 5. ACKNOWLEDGEMENTS

The authors would like to acknowledge the Mechanical Technical Department of IFES, Vitoria, Brazil and the financial support from Council for Scientific and Technological Development (CNPq) and Vale Company.

## 6. REFERENCES

Blessmann, J., 1988. "O vento na Engenharia Estrutural". Editora Universidade, Universidade Federal do Rio Grande do Sul.

Chang, C. and Meroney, R.N., 2003. "Concentration and flow distributions in urban street canyons: wind tunnel and computation data". *Journal of Wind Engineering and Industrial Aerodynamics*, Vol. 91, pp. 1141-1154.

Gayev, Y.A. and Savory, 1999. "Influence of street obstructions on flow processes within urban canyons". *Journal of Wind Engineering and Industrial Aerodynamics*, Vol. 82, pp. 89-103.

Gromke, C. and Ruck, B., 2007. "Influence of trees on the dispersion of pollutants in an urban street canyon – Experimental investigation of the flow and concentration field". *Atmospheric Environment*, Vol. 41, pp. 3287-3302.

Irwin, H.P., 1981. "The Design of Spires for Wind Simulation". Journal of Wind Engineering and Industrial Aerodynamics, Vol. 7, pp. 361-366.

Kim, J. and Baik, J., 2004. "A numerical study of the effects of ambient wind direction on flow and dispersion in urban street canyons using the RNG κ-ε turbulence model". *Atmospheric Environment*, Vol. 38, pp. 3039-3048.

Kim, Y.C.; Yoshida, A. Tamura, Y., 2012. "Characteristics of surface wind pressures on low-rise buildings located among large group of surrounding buildings". *Engineering Structures*, Vol. 35, pp. 18-28.

Louka, P., Belcher, S.E. and Harrison, R.G., 1998. "Modified street canyon flow". *Journal of Wind and Engineering and Industrial Aerodynamics*, Vol. 74, pp. 485-493.

Meroney R.N., Pavageau, M., Rafailidis, S., Schatzmann M., 1996. "Study of the line source characteristics for 2-D physical modeling of pollutant dispersion in street canyons". *Journal of Wind Engineering and Industrial Aerodynamics*, Vol. 62, pp. 37-56.

Oke, T.R., 1988. "Street design and urban canopy layer climate". Energy and Buildings, Vol. 11, pp. 103-113.

Vardoulakis, S., Fisher, B.E.A., Pericleous, K., Gonzalez-Flesca, N., 2003. "Modelling air quality in street canyons: a review". *Atmospheric Environment*, Vol. 37, pp. 155-182.

## 7. RESPONSIBILITY NOTICE

The authors are the only ones responsible for the printed material included in this paper.